



Neurons in Primary Motor Cortex Encode Hand Orientation in a Reach-to-Grasp Task

Chaolin Ma^{1,2} · Xuan Ma³ · Jing Fan² · Jiping He^{2,3,4,5}

Received: 8 October 2016 / Accepted: 20 February 2017 / Published online: 7 April 2017
© Shanghai Institutes for Biological Sciences, CAS and Springer Science+Business Media Singapore 2017

Abstract It is disputed whether those neurons in the primary motor cortex (M1) that encode hand orientation constitute an independent channel for orientation control in reach-to-grasp behaviors. Here, we trained two monkeys to reach forward and grasp objects positioned in the frontal plane at different orientation angles, and simultaneously recorded the activity of M1 neurons. Among the 2235 neurons recorded in M1, we found that 18.7% had a high correlation exclusively with hand orientation, 15.9% with movement direction, and 29.5% with both movement direction and hand orientation. The distributions of neurons encoding hand orientation and those encoding movement direction were not uniform but coexisted in the same region. The trajectory of hand rotation was reproduced by the firing patterns of the orientation-related neurons independent of the hand reaching direction. These results

suggest that hand orientation is an independent component for the control of reaching and grasping activity.

Keywords Primary motor cortex · Single neuron recording · Hand orientation · Non-human primate

Introduction

Reaching and grasping are tightly-choreographed movement sequences executed by the arm and hand in daily life. The timing of finger opening and closing when grasping must be coordinated with the arm reaching, and the posture of the hand must also be adapted to the size, shape, and/or orientation of the target object. Understanding how the brain coordinates the control of different components in such coupled movements is of great importance not only for fundamental neuroscience but also for developing effective cortically-controlled prosthetics or the neural rehabilitation of arm-hand function. Many studies have focused on identifying the anatomical locations and guiding physiological principles of the coordination of reaching and grasping [1, 2]. Other studies have focused on seeking significant features of human or monkey kinematics [3]. With electrophysiological recording in awake animals, it is possible to combine these two aspects and thoroughly investigate the relationship between cortical neuronal activity at the single-neuron level and movement parameters.

In a classic work on the neuronal control of reach-to-grasp, Jeannerod hypothesized that there are two channels: an extrinsic channel for the planning of reaching based on the object position in space, and another intrinsic channel for planning of grasping solely based on the object's shape and size. The hypothesis suggested that a central program

Chaolin Ma and Xuan Ma have contributed equally to this work.

✉ Chaolin Ma
chaolinma@ncu.edu.cn

✉ Jiping He
jiping.he@asu.edu

- ¹ Institute of Life Science and School of Life Science, Nanchang University, Nanchang 330031, China
- ² School of Biological and Health Systems Engineering, Arizona State University, Tempe, AZ 85287, USA
- ³ School of Automation, Huazhong University of Science and Technology, Wuhan 430074, China
- ⁴ Advanced Innovation Center for Intelligent Robots and Systems, Beijing Institute of Technology, Beijing 100081, China
- ⁵ Collaborative Innovation Center for Brain Science, Huazhong University of Science and Technology, Wuhan 430074, China

imposes temporal constraints so that the time of maximum grasp aperture and the onset of the low-velocity portion of the transport component are synchronous [4]. However, Marteniuk *et al.* showed that the correlation between the timing of the maximum grasp aperture and the onset of low-velocity movement was very weak at best, and might be influenced by object orientation [5]. They reported that object size affects both reaching time and peak velocity, and the purpose of reaching (hitting or grasping) also influences the velocity profile [6]. Hand orientation during reach-to-grasp is known to depend on the shape [7] and orientation [8, 9] of the object. Some models propose that object orientation and the corresponding control of hand orientation comprise a third important component of the reach-to-grasp process [10, 11]. Whether hand orientation for grasping is an independent component for the control of reach-to-grasp activity is unknown.

Separating the two channels for reaching and grasping was thought to be impossible from methods that cause neurological impairment [12]. However, investigation of cortical neuronal activity during reach-to-grasp has successfully separated them [13, 14]. Currently, it is widely accepted that cortical neurons encode information about reach direction and speed [15, 16]. Several other studies have demonstrated direct cortical control of a robot arm reaching for a target [17, 18].

In this study, we trained two monkeys to perform stereotyped reach-to-grasp tasks and made simultaneous electrophysiological recordings. We monitored cortical neuronal activity during reach-to-grasp to elucidate whether the possible hand orientation channel in M1 is an independent component for control of reach-to-grasp. We investigated whether the profile of hand rotation was represented by the firing patterns of the orientation-related neurons independent of the direction of hand reaching. By

exploring a wide area in M1 with moveable acute electrodes, we also investigated the spatial distribution of cortical neurons that encode hand orientation.

Materials and Methods

Animals

The electrophysiological data were collected from two male rhesus monkeys (*Macaca mulatta*): Monkey A and Monkey R, 4–6 years old. The experiments were strictly in compliance with the Guidelines for the Care and Use of Laboratory Animals of the National Institutes of Health, and were approved by the Animal Care and Use Committee of Arizona State University.

Experimental Apparatus and Task Protocols

A special experimental apparatus consisting of a horizontal board and a vertical panel was designed for training the monkeys to perform the tasks. A central holding pad was fixed on the horizontal board, and two rectangular target objects were mounted on the vertical panel (Fig. 1A). The distance between the central holding pad and the targets was 32 cm. Each target was directly connected to a programmable servomotor which could rotate 360° at up to 1100°/s. Lights for movement guidance were placed adjacent to the central holding pad and the target objects. Touch sensors were fitted on the surface of the central holding pad and on both sides of the targets for judging whether the monkey touched the right places.

The two monkeys were trained to reach out and grasp one of the two targets positioned on the vertical panel at three orientations (45°, 90°, or 135°). Each trial started

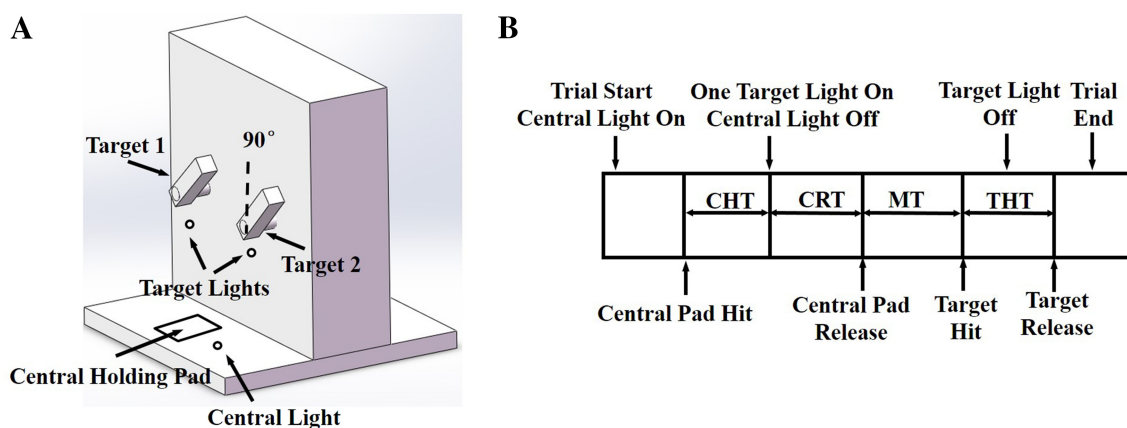


Fig. 1 Experimental apparatus and sequence of events in the reach-to-grasp task. **A** The experimental apparatus included a central light, a central holding pad, two target lights, and two target objects at three orientations (45°, 90°, 135°). The target orientation definition is

indicated. **B** The sequence of events and the trial epochs for the reach-to-grasp task in a typical successful trial. *CHT* center holding time, *CRT* cue reaction time, *MT* movement time, *THT* target holding time.

with the central light on for cueing the monkey to place its hand on the central holding pad. After a random center holding time (CHT) (300–700 ms), a target light was switched on, cueing the monkey to reach for the indicated target and make a whole-hand grasp using the power grip. The target light went off after the target was held for 100 ms or the allowed movement time expired. A trial was judged to be successful when the monkey grasped the target firmly using the power grip and made contact with both touch sensors; then several drops of water would be given as a reward. The monkey then returned its hand to the central holding pad and waited for the next trial.

The experimental events and time epochs for a typical successful trial are shown in Fig. 1B. The cue reaction time (CRT) was defined as the time from target light on to central pad release; the movement time (MT) was defined as the time from central pad release to target hit; and the target holding time (THT) was defined as the time from target hit to target release. The target orientation was switched in pseudo-random order with equal probability every 6 successful trials (3 trials to each target). The two targets were always oriented in parallel and the two target lights were presented in pseudo-random order with equal probability.

The monkeys were trained for 1 to 2 months until the proportion of successful trials every day exceeded 90%. Then they were prepared for electrode insertion and neuronal recording.

Surgery

In the surgery, the monkey was initially anesthetized with ketamine (8 mg/kg) and then maintained with isoflurane anesthesia (1.5%). To allow head restraint, a headpiece was first surgically mounted on the skull. At a second surgery, a single 23 mm × 20 mm chamber was mounted on the head to give access to record neuronal spikes in M1 of the left hemisphere. The four corners of the chamber were placed stereotaxically. After surgery the monkeys received a full course of antibiotic (20 mg/kg oxytetracycline, i.m.) and analgesic (10 µg/kg buprenorphine, i.m.).

Data Collection

After recovery from the chamber implant surgery, the animals were prepared for multiple-channel single-neuron recordings. A multi-electrode micro-drive (Thomas Recording, Giessen, Germany) was used to insert five independently controllable microelectrodes (quartz-insulated platinum-tungsten electrodes) through the dura into the M1 hand and arm area. Each electrode made one penetration each day. The recording depth was zeroed at the dura for every penetration. The coordinates of each

electrode were precisely calculated and recorded. When we drove the electrodes, the system provided the recording depth of each electrode, and when we picked up a neuron the depth was recorded. Since the experiment included several blocks per day, we monitored a large number of neurons. Neuronal signals were recorded using a Plexon Multichannel Acquisition Processor system (Plexon, Inc., Dallas, TX) at a sampling rate of 40 kHz/channel. Putative neuronal units were isolated using Offline Sorter software (Plexon, Inc.) for all channels using template-matching combined with the principal component method. Up to 4 units were discriminated on each channel.

During experiments, hand and arm movements were recorded by an optical motion-capture system (Optotrak, Northern Digital Inc., Waterloo, Canada). The three arm segments, hand, forearm, and upper arm, were marked with three infrared-emitting diodes (sampling rate 100 Hz) as described in previous studies [19].

Data Analysis

Cortical Data Analysis

Each trial was divided into four epochs: CHT, CRT, MT, and THT, and analyses were based on the average neuronal activity in each epoch. Epoch firing rates were computed for each cell by dividing the number of spikes recorded within each epoch by the epoch duration for each successful trial. The firing rate during the CHT was considered the baseline firing rate for each neuron.

Since the two targets were spaced symmetrically on the vertical plane, the reaching direction was the primary variant between the two targets. A significant target-variation in the neuronal activity would imply that the movement direction had an effect on the firing rate. Two-way analysis of variance (ANOVA) was used to evaluate whether changes in the average neuronal discharge in each experimental epoch were significantly modulated by hand orientation, or movement direction, or their interaction. Based on the results of two-way ANOVA, all of the recorded neurons were systematically classified as follows. The first step was to select task-related neurons. We defined a neuron as task-related if its average firing rate within any of the last three epochs (CRT, MT, and THT) was at least 2 standard deviations (SDs) greater than its baseline firing rate (the average rate within the CHT). The next step was conducted for all task-related neurons, and was based on the combination of epochs. For each neuron, we calculated the average firing rate during its active intervals (the epochs during which the firing rates were at least 2SDs greater than baseline). The firing rates for each cell were grouped by target orientation and movement direction, and tested with ANOVA. The numbers of

neurons exhibiting orientation, direction, and orientation-direction interaction effects were each counted. The latter effect can be understood as follows: a significant orientation-direction interaction effect was indicated when the orientation effect was not uniform between the two targets; conversely, a significant orientation effect without an interaction effect was indicated when the orientation effect was the same for the two targets.

To map the spatial distributions of the different types of neurons, a density was calculated at each penetration as the number of neurons related to orientation/direction divided by the total number of neurons recorded in that penetration. Then the densities for all penetrations were smoothed using a median filter, and the density contours for orientation-only neurons and direction-only neurons were plotted.

Kinematic Data Analysis

During the experiments, the 3-D positions of the markers attached on each arm segment were recorded by the tracking system, and the bone axes of each arm segment were defined by a set of right-handed orthogonal triads affixed to each segment. A baseline posture should be measured to align the marker positions and the bone axes when determining the rotation matrix from the bone axes to the marker axes. When measuring the baseline posture, the monkey held the elbow at 90° with the upper arm vertical and forearm horizontal in a parasagittal plane, and with the palm towards the central axis of the body. Thus the segment anatomical axes aligned with the global reference coordinates. The baseline rotation matrix from marker coordinates to the global coordinates equaled the rotation matrix from segment marker coordinates to segment bone coordinates.

Previous work in human subjects [19] showed that five angles are of interest in this task: hand pronation-supination, hand adduction-abduction, humeral rotation, forearm flexion-extension, and global hand rotation (hand rotation about the global coordinates). Among these, hand rotation in the global frame accounted for most of the variation and showed the largest range. Only global hand rotation was analyzed with the synchronous cortical data.

Reconstruction of Hand Orientation Trajectories

Reconstruction of hand orientation trajectories was computed from the neuronal data using linear and nonlinear regression methods separately. The interval of the neuronal spike data we used for the reconstruction was from 100 ms before movement onset to 200 ms after it, i.e., a 300-ms interval. This interval covered movement preparation, initiation, and execution. Specifically, the hand rotation angle

at time t_i was predicted from the neuronal responses (r_i^n) of multiple neurons (n) during a specific time bin in the past.

In the linear case, the optimal set of linear coefficients (f_i^n) was estimated that minimized the sum of squared difference between the predicted hand orientation (Y_i) and the actual hand orientation,

$$Y_i = \sum_{n=1}^N f_i^n r_i^n + C \quad (1)$$

where N is the total number of neurons incorporated in the reconstruction. The neuronal response of an individual neuron at one time point was computed as the number of spikes evoked in a time bin of width B . The two parameters N and B were systematically varied: N ranged from 1 to 25 neurons, and B ranged from 50 to 200 ms. The data set was randomly partitioned into two subsets. The performance of the linear model on each data set was estimated using half of the data set. A model was constructed leaving that set out as training data and using the remaining set as testing data.

In the nonlinear case, a two-layer artificial neural network was implemented using the MATLAB Neural Network Toolbox. The input layer consisted of N input nodes, corresponding to the responses of multiple cortical neurons. Log-sigmoid transfer functions were used between the input and the hidden layers. Linear transfer functions were used between the hidden and the output layers. The output layer consisted of one node, representing the predicted hand orientation Y_i at time t_i . A gradient descent with an adaptive learning rate back-propagation training algorithm was used for network parameter identification. This showed that three artificial neurons in the hidden layer was optimal for the network. For each target, the data set was randomly partitioned into a training set (50% of the data), a validation set (22% of the data), and a test set (28% of the data). For the training process, the parameters of the network were obtained through the training algorithm described above to minimize the sum of squared difference between the actual and predicted hand orientations. To prevent overfitting, the sum of squared error for the validation set was computed after each training epoch, and the training was stopped when the value began to increase. The test set was then used to estimate the generalization performance of the trained network.

Results

Behavioral Results

Both monkeys were well trained before electrode implantation. When neuronal recordings commenced, both

monkeys achieved success in >90% of task trials. The durations of each epoch (CHT, CRT, MT, and THT) for both movement directions and object orientations are listed in Table 1.

Hand Rotation Starts in Parallel with Reaching

According to the experimental paradigm, hand orientation was determined by the three target orientations: 45°, 90°, and 135° measured clockwise from palm down (Fig. 2A), and arm-reaching direction was determined by the 2 target positions: left and right. The transport velocity profiles showed no dependence on target orientation (Fig. 2B). The

arm reaching and hand rotation were coordinated during the reach-to-grasp task.

M1 Neurons Code for Hand Orientation and Reaching Direction

During the reach-to-grasp task, a total of 2235 M1 neurons were recorded from the two monkeys (979 from monkey R and 1256 from monkey A). Of these, 1676 were correlated with hand orientation and/or reaching direction.

The neurons correlated with hand orientation only and independent of reaching direction were designated as orientation-only neurons (Fig. 3A). By comparing a neuron's

Table 1 Summary of average epoch durations (\pm SD) for each monkey at each condition.

Monkey	Direction	Orientation (°)	CHT	CRT	MT	THT
Monkey R	Left	45	523 \pm 112	267 \pm 42	338 \pm 42	128 \pm 25
		90	514 \pm 109	256 \pm 74	371 \pm 41	120 \pm 13
		135	527 \pm 122	243 \pm 50	357 \pm 45	123 \pm 23
	Right	45	534 \pm 139	261 \pm 74	364 \pm 77	118 \pm 19
		90	505 \pm 131	248 \pm 67	354 \pm 62	127 \pm 13
		135	521 \pm 124	252 \pm 70	347 \pm 43	120 \pm 22
Monkey A	Left	45	498 \pm 122	210 \pm 66	365 \pm 38	105 \pm 16
		90	505 \pm 96	206 \pm 48	345 \pm 49	116 \pm 15
		135	494 \pm 105	198 \pm 57	340 \pm 47	112 \pm 13
	Right	45	490 \pm 110	207 \pm 35	348 \pm 24	115 \pm 16
		90	493 \pm 100	195 \pm 52	334 \pm 37	108 \pm 20
		135	492 \pm 134	206 \pm 37	350 \pm 30	105 \pm 15

CHT center holding time, CRT cue reaction time, MT movement time, THT target holding time (in ms).

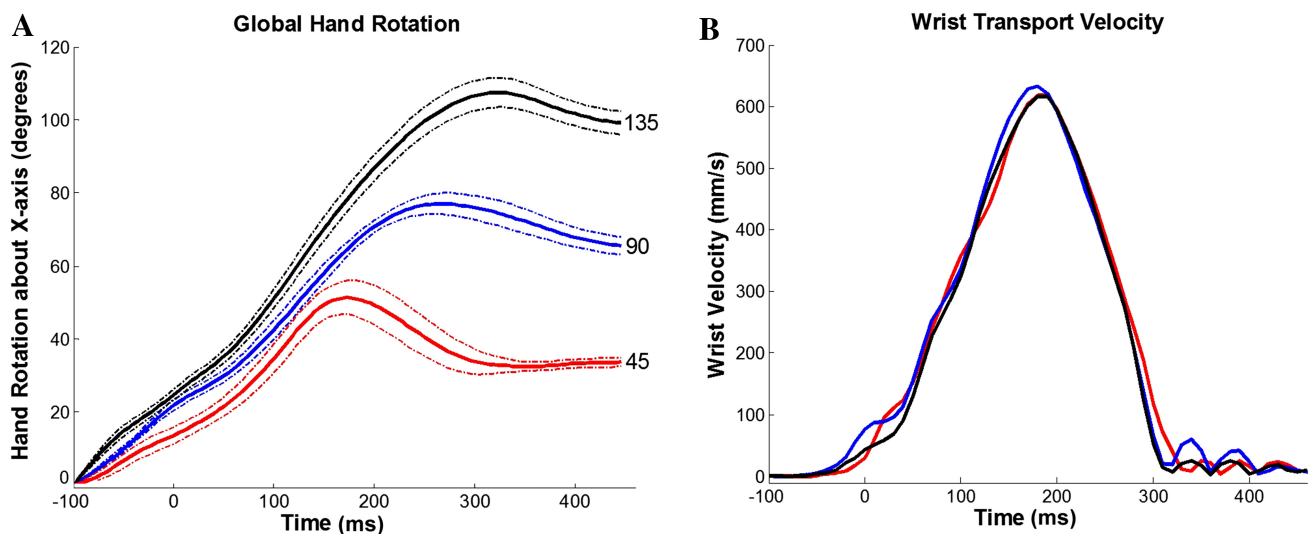


Fig. 2 Dependence of movement parameters on target orientation. **A** Averaged hand rotation trajectories (solid curves) \pm SDs (dashed curves) during movements to targets oriented at 45° (red), 90° (blue), and 135° (black). Each solid curve was averaged from all trials of movements of monkey R to the same target fixed at the same orientation. Time zero is aligned on central pad release. **B** Averaged

wrist transport velocity profiles to the same target at different orientations. Color index as in A. Time zero is also aligned on central pad release. The trajectory indicated that the reaching (transport) component was not influenced by the target orientation, but the hand orientation was modulated from movement initiation.

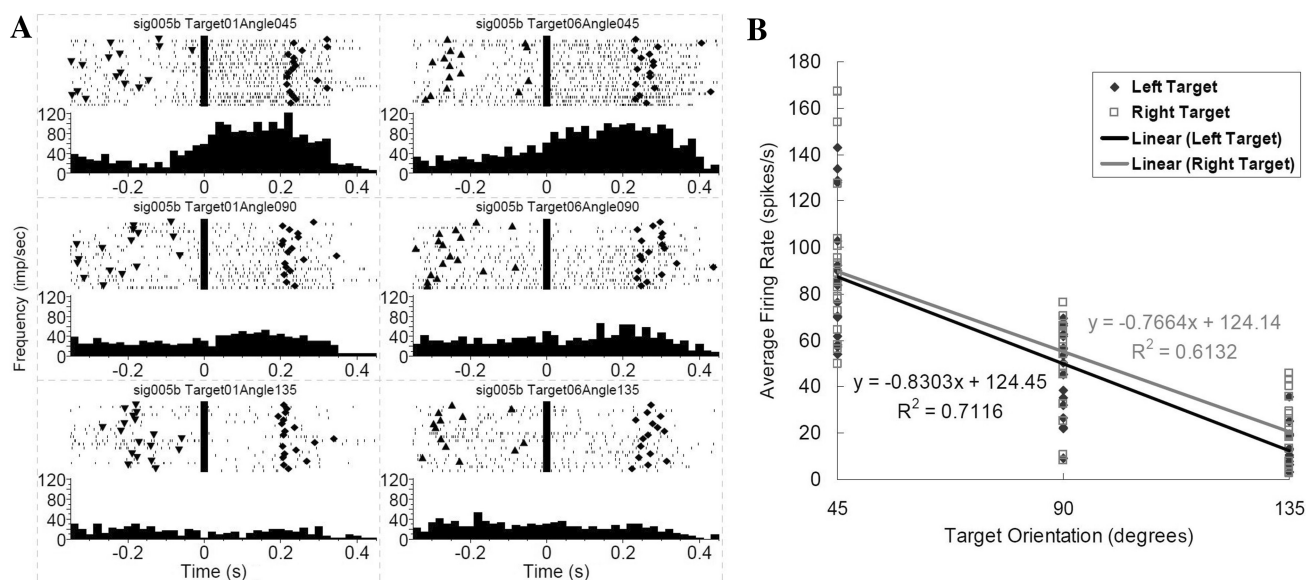


Fig. 3 Example of a motor cortical neuron encoding target orientation only. **A** Peri-event rasters and histograms during reach-to-grasp the target oriented at three different angles. *Left column* cell activity during movement to the left target; *right column* cell activity during movement to the right target. The three rows correspond to 45°, 90°, and 135° target orientations. Each raster illustrates the discharge pattern of the cell during 18 trials of movements to each target fixed at

firing rate from ~100 ms before movement onset (i.e. with the hand at the central holding pad) to the time when target grasping was completed, we found that hand orientation changed the overall level of discharge before, during and after movements (two-way ANOVA; effect of hand orientation, $P < 0.05$) independent of target location or movement direction (effect of target location, $P > 0.05$).

For example, when the average firing frequency of the neuron in Fig. 3A during the complete movement period in each trial was calculated and plotted *versus* target orientation for all successful grasps (Fig. 3B), it showed a high correlation with the target orientation regardless of the target location or movement direction. A successful grasp ensured that the hand orientation at the grasp was in alignment with the target orientation. The changes in the average firing rate between movements to targets oriented at 45° and 135° were 75 spikes/s for the left target and 69 spikes/s for the right target. The cortical activity during movements to the 45° target had the greatest firing frequency (average firing rate 87.09 spikes/s for the left target and 89.65 spikes/s for the right target). However, this was not true for every orientation-only neuron. For some other neurons, movements to targets at a larger orientation angle (90° or 135°) corresponded to a higher firing frequency. Following the naming tradition for motor neurons, we defined the orientation angle for which a neuron had the highest firing frequency as the preferred orientation for that neuron.

the same orientation. The rasters are ordered by trial sequence. Time zero is aligned on the central pad release (movement onset). *Triangles* target light on; *diamonds* target hit. The histograms were calculated with a bin-width of 20 ms. **B** Relationship between average firing rate and target orientation for this orientation-only neuron approximated by a linear regression.

A second group of neurons showed correlation with movement direction only, independent of target orientation or hand rotation. This is consistent with known results that the activity of a large population of motor cortical neurons is highly correlated with movement direction [15, 16, 18]. The discharge frequency of this type of neuron during movement to one of the targets was higher (ANOVA, effect of movement direction, $P < 0.05$) than that to the other parameters, and this difference was found for all three target orientations (Fig. 4).

The third type of neuron showed a high correlation with both target orientation and movement direction (ANOVA, $P < 0.05$). Regarding the effect of target orientation, there was a significant change in the overall level of activity among movements to targets at different orientations (Fig. 5A). Regarding the effect of movement direction, the neuronal firing frequency during movement to the left target was always ~20 spikes/s higher than that to the right target (Fig. 5A), despite the similar positive linear relationship of firing rate with target orientation (Fig. 5B).

The fourth type of neuron was found to have a significant orientation-direction interaction (ANOVA, interaction effect of orientation and direction, $P < 0.05$). The target location or movement direction changed the neuronal discharge pattern on orientation (Fig. 6A). In this example, for the left target, the neuron's discharge frequencies during movements to 45° and 90° were clearly higher than that

Fig. 4 Example of a motor cortical neuron encoding target direction only. Peri-event rasters and histograms of a neuron encoding target direction only, as in Fig. 3A. *Left column* activity during movement to the left target; *right column* activity during movement to the right target.

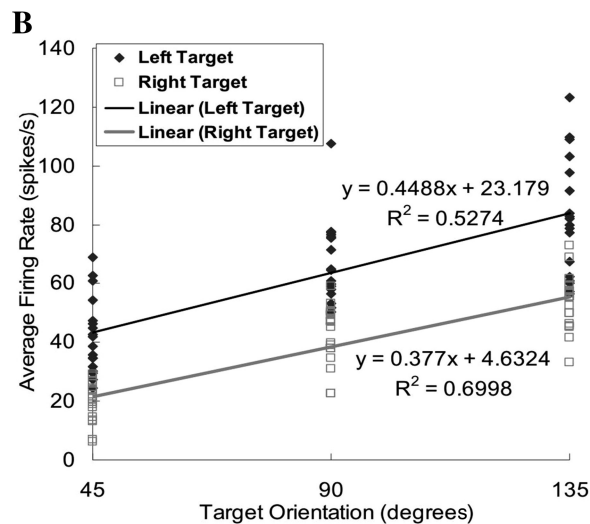
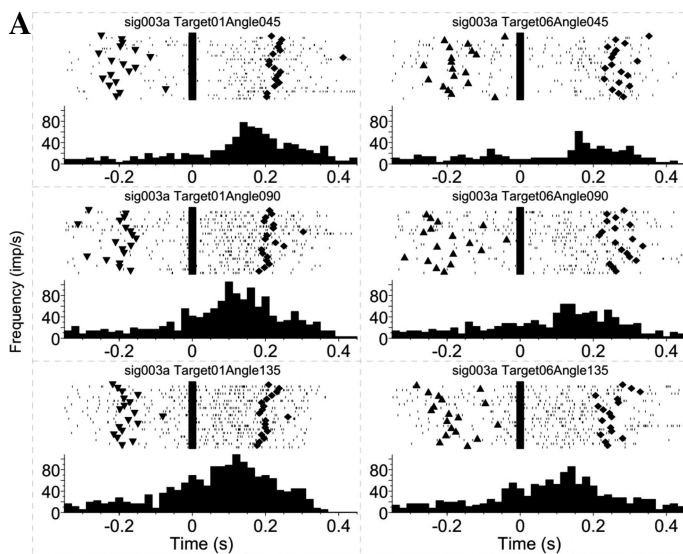
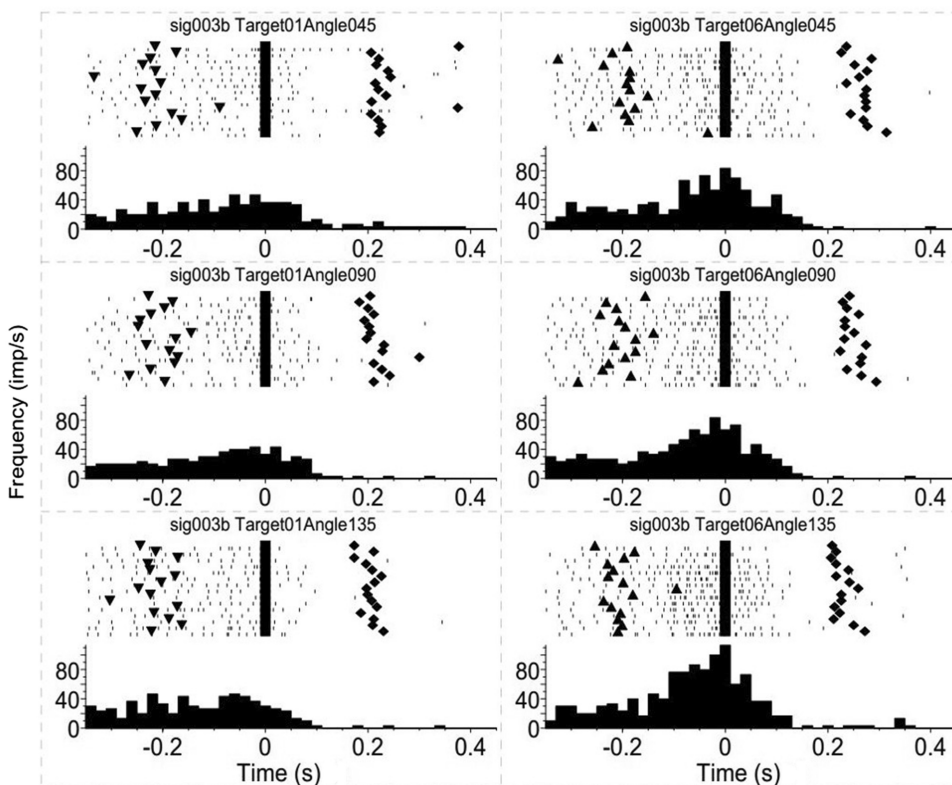


Fig. 5 Example of a motor cortical neuron encoding both target orientation and movement direction. **A** Peri-event rasters and histograms of a neuron encoding both target orientation and movement direction, as in Fig. 3A, showing a positive correlation

during movements to 135°. However, for the right target, movements to the 135° target corresponded to the highest discharge frequency. The firing frequency during movements to the left target had a negative linear relationship with target orientation, while the firing frequency during

with hand orientation for both targets but significantly different average firing rates for the left and right targets. **B** Two significantly different positive linear relationships between firing rates and target orientations for the left and right targets of the neuron shown in (A).

movement to the right target had a positive linear relationship with target orientation (Fig. 6B). These results suggested that the movement direction reversed the proportional relationships of the firing frequency with the orientation angles.

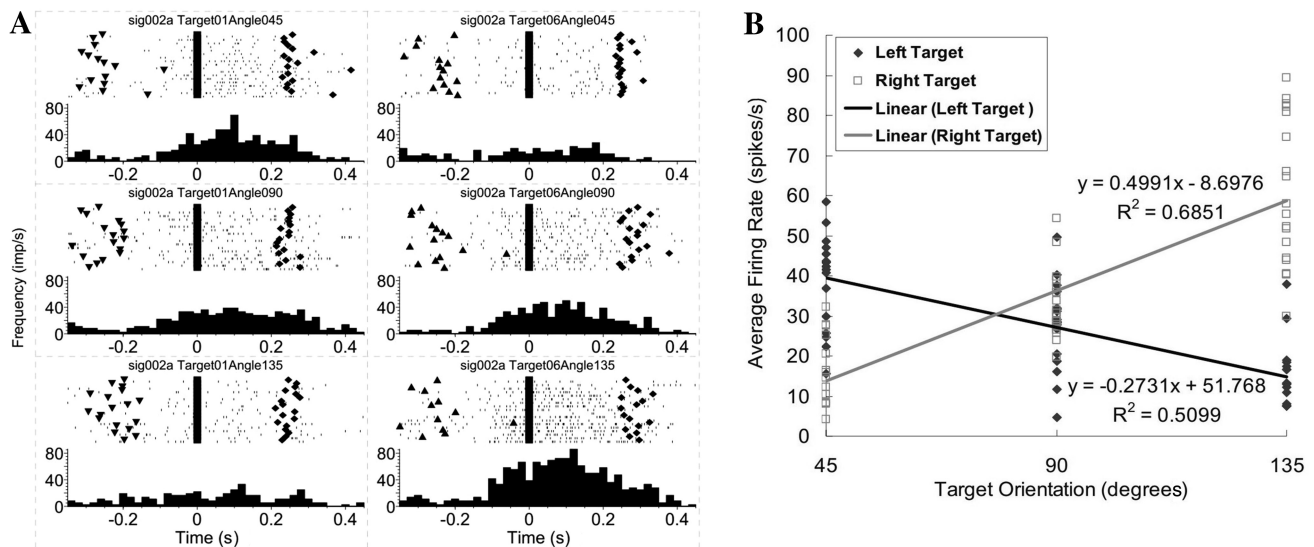


Fig. 6 Example of a motor cortical neuron encoding an orientation-direction interaction. **A** Peri-event rasters and histograms of a neuron encoding an orientation-direction interaction, as in Fig. 3A. Shown is an opposite correlation between average firing rates and target orientations when reaching different target locations (negative for left

target and positive for right target). **B** Positive and negative linear relationships exist between the firing rates and the target orientations during movement to the left and right targets for the neuron shown in (A).

Overlapping Distributions of Cortical Motor Neurons Coding for Hand Orientation and Reaching Direction

By summarizing the neuronal coding, we found that 19% of the cells (313 of 1676) were correlated with target orientation only, 16% (266 of 1676) with movement direction only, 11% (186 of 1676) with both target orientation and movement direction, and 18% (309 of 1676) with an interaction of orientation and direction (Fig. 7A). The remaining neurons, though showing modulation during the task, were not directly correlated with either hand orientation or reaching direction.

The spatial distribution of recorded neurons encoding different orientation angles was not uniform. More neurons showed a preferred orientation for the supinated angle 135° (52% for Monkey R and 55% for Monkey A) than for the other two orientations (26% for 45° and 22% for 90° from monkey R, 23.5% for 45° and 21.5% for 90° from Monkey A). The overall distribution was similar for both target directions in the two monkeys.

If the uneven distribution of preferred orientations was caused by recording sample bias, we would find neurons in a specific cortical area preferring a particular orientation. The spatial distribution of the orientation-only neurons was plotted according to their orientation preference (Fig. 7B, composite of both monkeys, Fig. 7C for monkey R and Fig. 7D for monkey A). No clustering of neurons preferring a particular orientation was evident in a specific area,

although the neurons recorded in the same penetration tend to have a similar orientation preference.

To map the cortical distributions of the orientation-only neurons and the direction-only neurons, we compared their density contours (Fig. 8), which revealed the areas of highest clustering density. Based on these contours, a common hot area for both the orientation-only and the direction-only neurons in the M1 area at the level of the arcuate sulcus spur was identified in both monkeys. Meanwhile, there was no evident difference in the penetration depths between the two types of neurons (Fig. 8B–D).

Estimating Control Command for Reach-to-Grasp from Recorded Neuronal Activity

Simple multi-regression and a two-layer artificial neural network were used to predict the hand orientation with only a handful of neurons from the recorded population. We varied the bin size B (50, 100, 150, and 200 ms) used to calculate the neuronal firing rate to define the optimal bin size for reconstructing the hand orientation trajectory (Fig. 9). The results showed that 100-ms bins generated the least sum of squared error for both targets, and that using more neurons produced a more reliable reconstruction. Therefore, the spike counts of each incorporated neuron were calculated in a 100-ms window with a sliding step of 20 ms.

Hand orientation trajectories were reconstructed using multiple linear regression (Fig. 10A) and a nonlinear

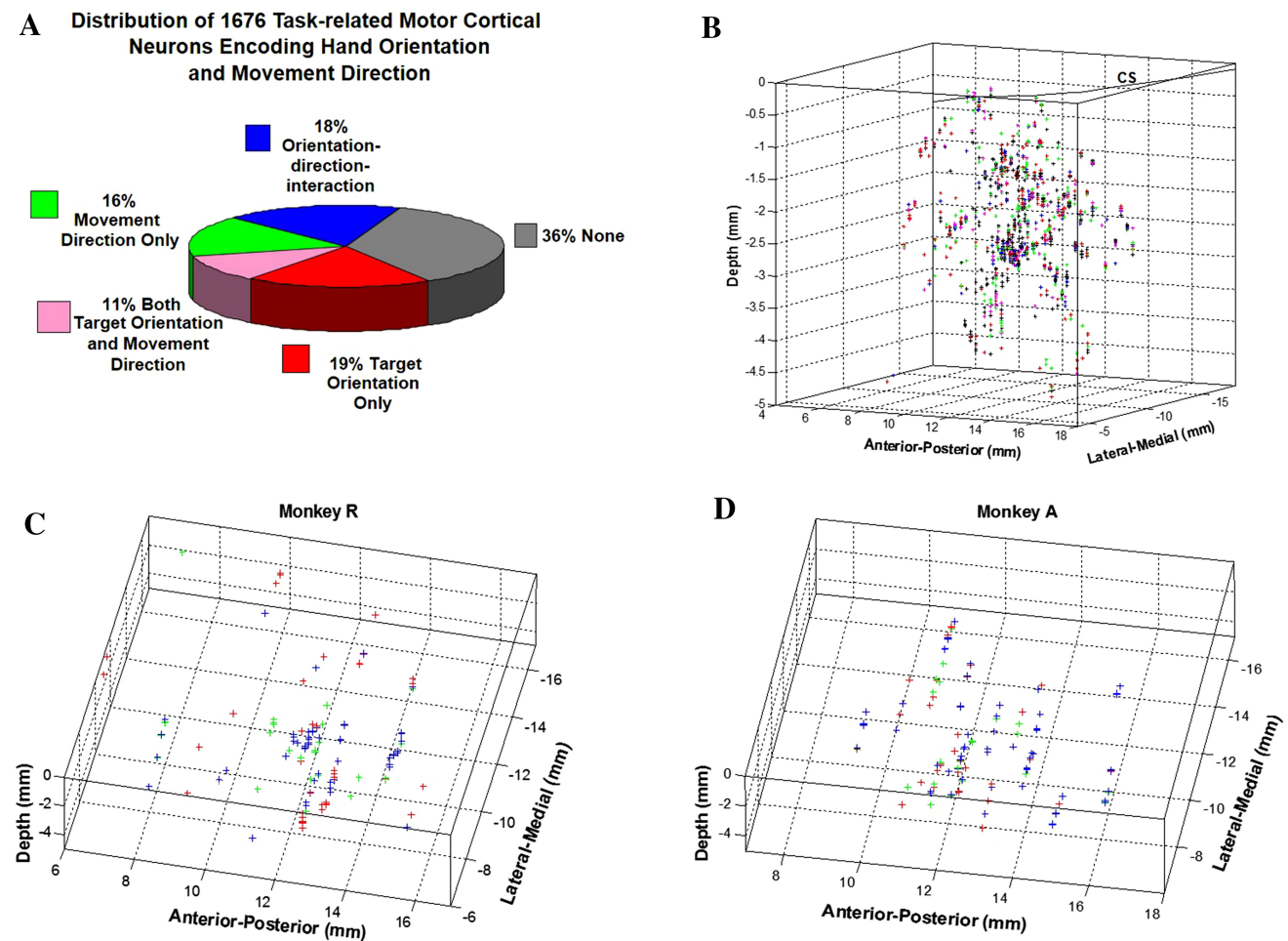


Fig. 7 Distribution of 1676 task-related motor cortical neurons encoding target orientation and movement direction. **A** Pie chart showing the distribution of cortical encoding. **B** 3-D map of the 1676 task-related neurons. Each *cross* represents a single neuron; different colors indicate different orientation preferences: 45° (red),

90° (green), and 135° (blue). There was no clear topographic arrangement of neurons for different orientations as shown in (C, D): 141 orientation-only neurons from Monkey R and 172 from Monkey A.

artificial neural network (Fig. 10B). The nonlinear artificial neural network approach produced a more accurate estimate than the linear regression method. It should also be noted that there was not much difference between the linear and nonlinear methods in the early stage of the reconstructed movements, and both methods predicted the hand orientation trajectories quite well (0–150 ms). In contrast, in the later stage (150–300 ms), the nonlinear method was clearly more powerful in predicting movements more consistently than the linear method. This may be because at the later stage, the reach-to-grasp movement is more complicated than at the early stage, in that several events occur simultaneously at this stage, such as adjusting the final hand orientation, reducing the transport speed, and adjusting the aperture or starting to close the fingers. In this situation, the powerful nonlinear artificial neural network method works better to process more information.

Discussion

In this study, we investigated the neuronal mechanisms by which M1 neurons encode the control of hand orientation in a reach-to-grasp task. Electrophysiological recordings were conducted on two monkeys, and a number of task-related neurons were detected. Data analyses were based on the firing rate patterns of neurons.

In the analysis, the firing rate during the CHT was considered the baseline rate for each neuron. The firing rates of 152 neurons (6.8% of 2235) within the CHT were significantly altered by target orientation, and these neurons were classified into the non-movement-related group, since the monkey's hand was at rest on the central holding pad during the CHT, the target had not been presented, and movement had not started. These neurons might play a key role in planning the movement for

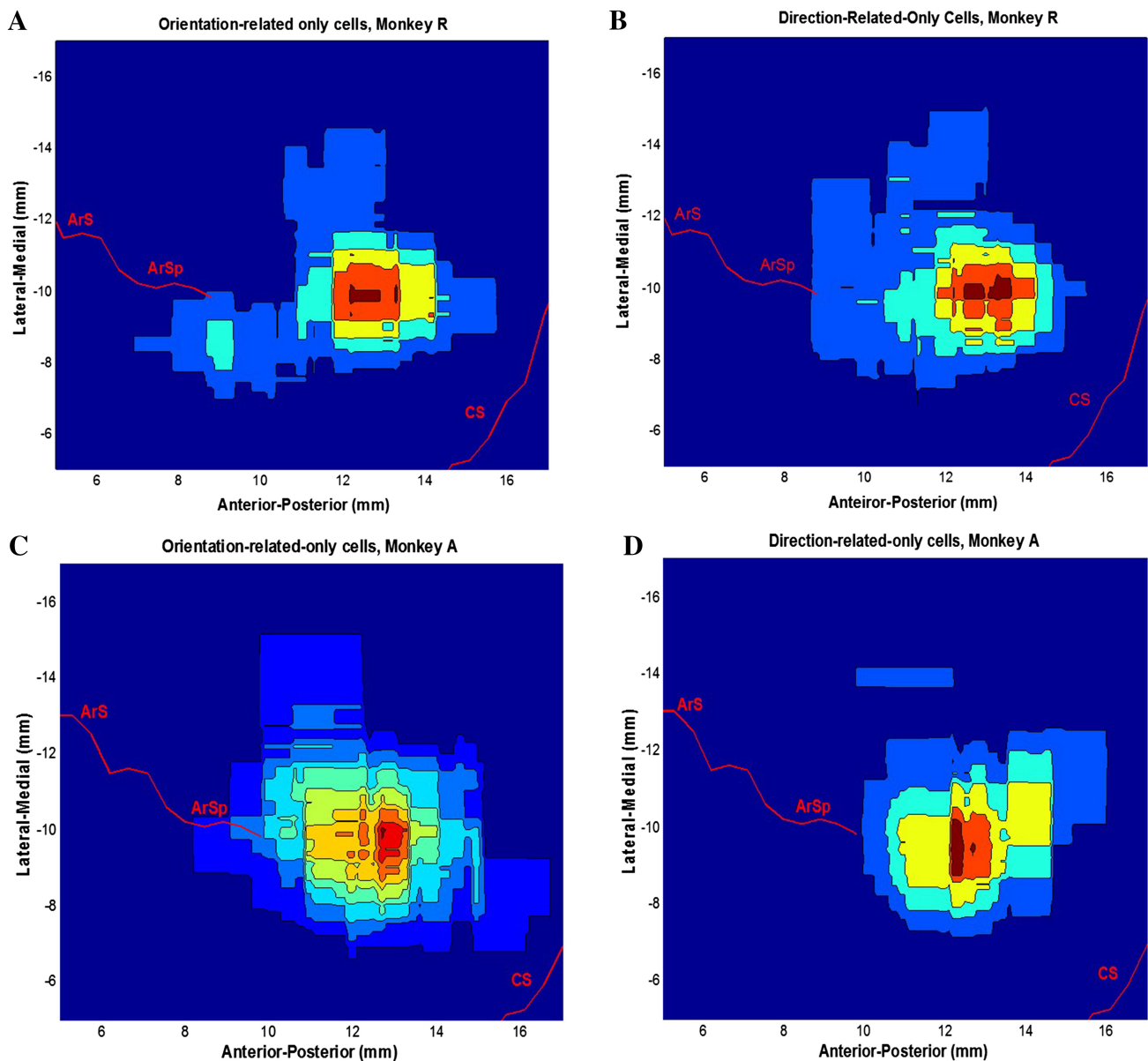


Fig. 8 Density contours of orientation-only and direction-only cells. **A, C** Density contours of orientation-only cells in the chamber coordinates. **B, D** Direction-only cells in the chamber coordinates.

reach-to-grasp, such as visuo-motor integration. However, it was not the focus of this investigation and the number was small.

Similarly, we also excluded 42 (1.9%) likely sensory neurons, which showed significantly higher firing frequencies during the CHT, CRT, and THT when the hand was either touching the central holding pad or holding the target, but lower firing frequencies during the MT when there was no cutaneous input.

The next step was to select task-related neurons using the criterion that the average firing rate within any of the last three epochs (CRT, MT, or THT) was at least 2SDs greater than the baseline rate. Besides the above two types

of neurons, 365 (16.3%) showed no significant increase in discharge frequency during any of the last three epochs and were classified as non-task-related. The remaining 1676 neurons (75%) were considered to be task-related and further analyzed. The average firing rate of each task-related neuron during the active intervals was grouped by target orientation and movement direction.

We fixed the initial hand position and final target location to keep the movement directions stable, and studied the reach-to-grasp movements to targets oriented at three different angles. One special feature of the experiment was that the hand orientation was determined by the target orientation. Our findings showed that a significant number

Fig. 9 Decoding error as a function of number of orientation-related motor cortical neurons and bin size. Sum of squared error calculated from the multiple linear regression results of 1–25 motor cortical neurons for the left (A) and right (B) targets. The four curves on each plot represent the bin sizes 50, 100, 150, and 200 ms.

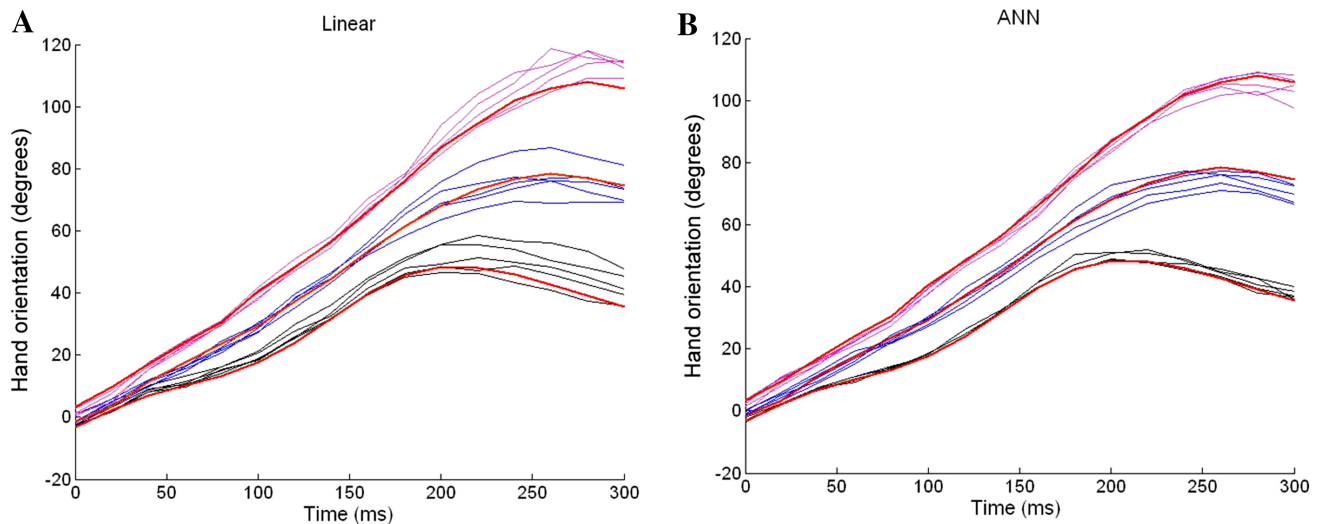
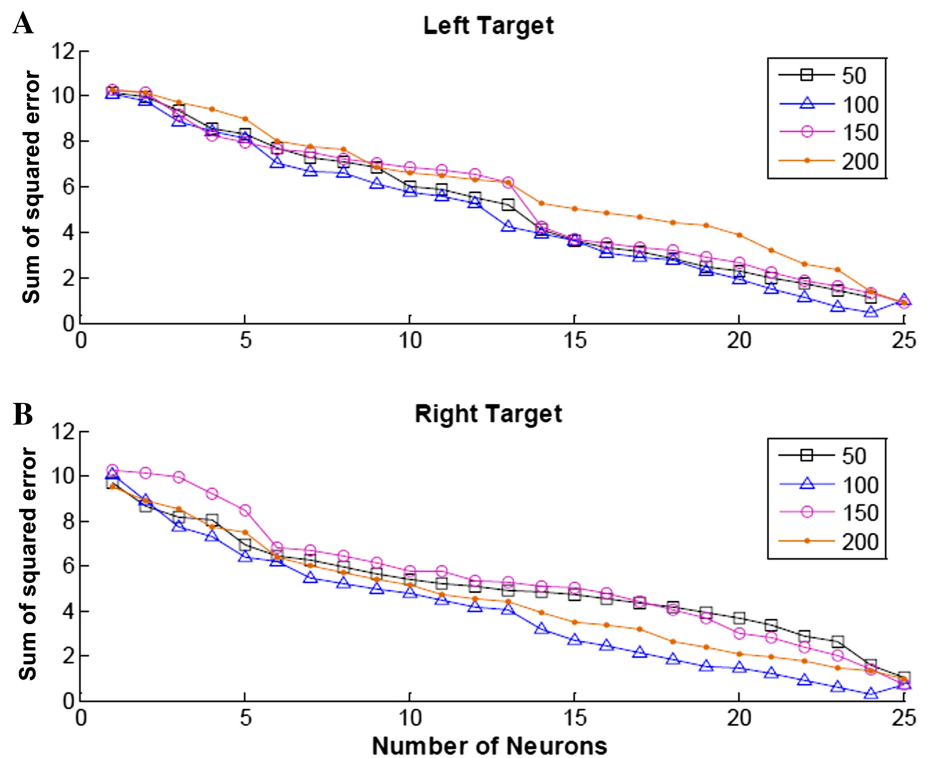


Fig. 10 Reconstruction of hand orientation trajectories from motor cortical ensembles. **A** Hand orientation trajectories reconstructed using the multiple linear regression method. We used 50% of the data as training data, and the other 50% as the test data. Here, we only

of cortical motor neurons contributed to the control of hand orientation. In addition, changes in hand orientation altered the discharge activity of cortical motor neurons before, during, and after reach-to-grasp movements.

The present work revealed that the discharge patterns of a significant number of M1 motor neurons correlated with hand orientation and were independent of target location during

plotted the results from 15 trials for comparison with plot (B). Color index: 45° (black), 90° (blue), and 135° (purple); red dashed lines averaged actual hand orientation trajectories. **B** Hand orientation trajectories reconstructed using the artificial neural network method.

reach-to-grasp movements. This contradicts the suggestion that arm transport and hand orientation do not constitute independent visuomotor channels [20]. Our results suggest that hand orientation is an important and independent control parameter during three-dimensional reach-to-grasp.

In addition, a majority of the orientation-only neurons started to show the orientation preference ~ 100 – 200 ms

prior to movement onset. This result supports our previous conclusion that visual information related to object orientation is taken into account at the very beginning of a prehension movement [19]. This result is compatible with previous findings that the representation of a visual target in extrapersonal space has to be transformed into a kinesthetic representation of arm segment orientation before a goal-directed movement can be implemented [21]. Our finding suggests that the final posture to be reached is a control variable specified by the brain in advance of the movement. This finding is also consistent with the suggestion that arm posture or configuration has a strong influence on motor cortical neuronal activity [22].

Previous studies [15, 23] have shown that single motor cortical neurons commonly engage several motor neuronal pools and that, within a particular engaged pool, the connections of the motor cortical neurons are widespread [23]. This one-to-many relation between motor cortical neurons and motor neuronal pools, and the reasonable assumption that a particular motor cortical neuron can engage different pools at different strengths, might explain our finding that the preferred orientations of single motor cortical neurons differ among different neurons. Similar to the results revealed by other studies concerning arm-reaching experiments, different single motor cortical neurons had various preferred directions. The results of those studies suggested that single neurons might be associated with groups of muscles, such that a particular neuron might engage several motor neuronal pools in a weighted fashion.

Our results showed that a significant number of motor cortical neurons had a high correlation with target orientation, including 19% encoding orientation only, 11% encoding both orientation and direction, and 18% encoding an interaction between orientation and direction, among the total 1676 recorded neurons. Meanwhile, different neurons had different orientation preferences. This property was similar to the neuronal coding of reaching movement direction, for which it was shown that single neurons were tuned with respect to the direction of the reaching movement and, therefore, could be assigned a preferred direction for which neuron activity was highest; preferred directions differed among neurons and ranged throughout the directional continuum.

We found that separate neuronal populations showed an explicit innervation relationship to hand orientation and movement direction. This finding indicated that hand orientation is an important control parameter during reach-to-grasp in parallel with movement direction and velocity. The overlapping distributions of these neurons suggested that, for practical applications in brain-machine interfaces, the general information for reach-to-grasp could be obtained together from the same motor cortical region.

In summary, our findings from electrophysiological recordings suggest that hand orientation is an independent component for the control of reaching and grasping. By plotting the density contours of the different types of neurons, we showed that the distributions of neurons encoding hand orientation and those encoding movement direction are not uniform but coexist in the same region of motor cortex. Meanwhile, the trajectory of hand rotation can be reproduced accurately independent of the hand reaching direction, which also supports the hypothesis of an independent cortical control channel for orientation.

Acknowledgements This work was supported by the National Natural Science Foundation of China (61233015 and 31460263), and the National Basic Research Development Program (973 Program) of China (2013CB329506). We appreciate the collaboration with Dr. Steve Helms Tillery and Dr. Yury Shimansky in the Neural Control Laboratory at Arizona State University, USA.

References

1. Georgopoulos AP, Kalaska JF, Caminiti R, Massey JT. On the relations between the direction of two-dimensional arm movements and cell discharge in primate motor cortex. *J Neurosci* 1982, 2: 1527–1537.
2. Kawashima R, Roland PE, O' Sullivan BT. Fields in human motor areas involved in preparation for reaching, actual reaching, and visuomotor learning: a positron emission tomography study. *J Neurosci* 1994, 14: 3462–3474.
3. Georgopoulos AP, Kalaska JF, Massey JT. Spatial trajectories and reaction times of aimed movements: effects of practice, uncertainty, and change in target location. *J Neurophysiol* 1981, 46: 725–742.
4. Jeannerod M. The formation of finger grip during prehension: cortically mediated visuomotor pattern. *Behav Brain Res* 1986, 19: 99–116.
5. Marteniuk RG, Leavitt JL, MacKenzie CL, Athenes S. Functional relationships between grasp and transport components in a prehension task. *Human Movement Science* 1990, 9: 149–176.
6. Marteniuk R, MacKenzie C, Jeannerod M, Athenes S, Dugas C. Constraints on human arm movement trajectories. *Can J Psychol* 1987, 41: 365–378.
7. Klatzky R, Fikes T, Pellegrino J. Planning for hand shape and arm transport when reaching for objects. *Acta Psychol (Amst)* 1995, 88: 209–232.
8. Desmurget M, Prablanc C. Postural control of three-dimensional prehension movements. *J Neurophysiol* 1997, 77: 452–464.
9. Mamassian P. Prehension of objects oriented in three-dimensional space. *Exp Brain Res* 1997, 114: 235–245.
10. Soechting J, Flanders M. Parallel, interdependent channels for location and orientation in sensorimotor transformations for reaching and grasping. *J Neurophysiol* 1993, 70: 1137–1150.
11. Torres E, Zipser D. Reaching to grasp with a multi-jointed arm computational model. *J Neurophysiol* 2002, 88: 2355–2367.
12. Lang C, Wagner J, Edwards D, Sahrman S, Dromerick A. Recovery of grasp versus reach in people with hemiparesis poststroke. *Neurorehabil Neural Repair* 2006, 20: 444–454.
13. Georgopoulos A. Cortical Mechanisms Subservient Reaching. *Ciba Found Symp* 1987, 132: 125–141.

14. Lemon R, Johansson R, Westling G. Modulation of corticospinal influence over hand muscles during gripping tasks in man and monkey. *Can J Physiol Pharmacol* 1996, 74: 547–558.
15. Georgopoulos A, Kettner R, Schwartz A. Primate motor cortex and free arm movements to visual targets in 3-Dimensional space. *J Neurosci* 1988, 8: 2928–2937.
16. Schwartz A. Direct cortical representation of drawing. *Science* 1994, 265: 540–542.
17. Donoghue J. Connecting cortex to machines: recent advances in brain interfaces. *Nat Neurosci* 2002, 5: 1085–1088.
18. Taylor D, Tillery S, Schwartz A. Direct cortical control of 3D neuroprosthetic devices. *Science* 2002, 296: 1829–1832.
19. Fan J, He J, Tillery S. Control of hand orientation and arm movement during reach and grasp. *Exp Brain Res* 2006, 171: 283–296.
20. Desmurget M, Prablanc C, Arzi M, Rossetti Y, Paulignan Y, Urquizar C. Integrated control of hand transport and orientation during prehension movements. *Exp Brain Res* 1996, 110: 265–278.
21. Tillery S, Flanders M, Soechting J. A coordinate system for the synthesis of visual and kinesthetic information. *J Neurosci* 1991, 11: 770–778.
22. Scott S, Kalaska J. Reaching movements with similar hand paths but different arm orientations. *J Neurophysiol* 1997, 77: 826–852.
23. Lemon R, Mantel G, Muir R. Corticospinal facilitation of hand muscles during voluntary movement in the conscious monkey. *J Physiol* 1986, 381: 497–527.